

Supporting Information for

Fully Solar-Powered Photoelectrochemical Conversion for Simultaneous Energy Storage and Chemical Sensing

*Yongcheng Wang[†], Jing Tang[†], Zheng Peng[†], Yuhang Wang[†], Dingsi Jia[†], Biao Kong[†],
Ahmed A. Elzatahry^{*‡}, Dongyuan Zhao[†], and Gengfeng Zheng^{*†}*

[†] Laboratory of Advanced Materials, Department of Chemistry, Fudan University, Shanghai, 200433, People's Republic of China

[‡]Department of Chemistry, King Saud University, Riyadh 11451, Riyadh, Saudi Arabia

[‡] Polymer Materials Research Department, Advanced Technology and New Materials Research Institute, New Borg El-Arab City, Alexandria, Egypt

* Address correspondence to: gfzheng@fudan.edu.cn.

Methods

Synthesis of the TiO₂ NW/NiO nanoflakes arrays. TiO₂ NW arrays were synthesized by a modified hydrothermal method, in which a fluorine-doped tin oxide (FTO) substrate was used as the substrate for TiO₂ NW growth. After the growth, NiO nanoflakes were prepared by a modified chemical bath deposition method. Briefly, 16.5 g of NiSO₄·6H₂O, 2 g of K₂S₂O₈ and 5 mL of aqueous ammonia (25-28%) were added into 200 mL of H₂O, then the FTO substrate containing the as-grown TiO₂ NW arrays was immersed in the solution and stirred for 30 min. The sample was then taken out and rinsed with water and annealed at 200 °C in argon for 1.5 h.

Synthesis of Si NW/Pt arrays. Si NW arrays were prepared by a metal-assisted etching method. Single crystalline, 0.01 Ω·cm *p*-Si (100) wafers were cleaned, and immersed in a solution contained 0.136 g of AgNO₃, 10 mL of aqueous HF and 30 mL of H₂O to form Ag nanoparticles, followed by etching in the solution contained 0.8 mL of H₂O₂, 10 mL of aqueous HF and 30 mL of H₂O for 30-60 min. After etching, the Si NW arrays were immersed in a bath of concentrated nitric acid for 30 min to remove Ag. Pt nanoparticles were deposited onto Si NWs surfaces by an electroless metal deposition in a solution containing 2.5 mL of H₂PtCl₆ (20 mM) solution, 1 mL of aqueous HF and 50 mL of H₂O for 10 min.

PEC measurements. Photocurrent measurement was carried out in a two-electrode configuration with the TiO₂/NiO photoanode and the Si/Pt photocathode in a 0.5 M Na₂SO₄ solution, by a CHI660D electrochemical workstation. The open circuit potential versus time measurement was carried out under the same configuration. Discharge measurement was carried out in a three-electrode configuration with TiO₂/NiO as the working electrode, Pt foil as the counter electrode, and Ag/AgCl as the reference electrode. A 0.5 M Na₂SO₄ was used as the electrolyte. The discharge measurement was performed by galvanostatic discharge tests. The specific capacitance was calculated by: $C = I * \Delta t / (M * \Delta V)$, where C (F g⁻¹) is the specific capacitance, I (A), Δt (s), M (g), and ΔV (V) represent the discharge current, the total

discharge time, the mass of active materials, and the potential drop during discharge, respectively.

Sensing measurements. In the solar energy driving mode, the TiO_2/NiO photoanode and the Si/Pt photocathode are connected in the aforementioned 2-electrode configuration. In the pseudocapacitive energy driving mode, a 3-electrode configuration is used, with the TiO_2/NiO photoanode, a Pt foil and a Ag/AgCl as the working, counter and reference electrodes, respectively.

Supporting Figures

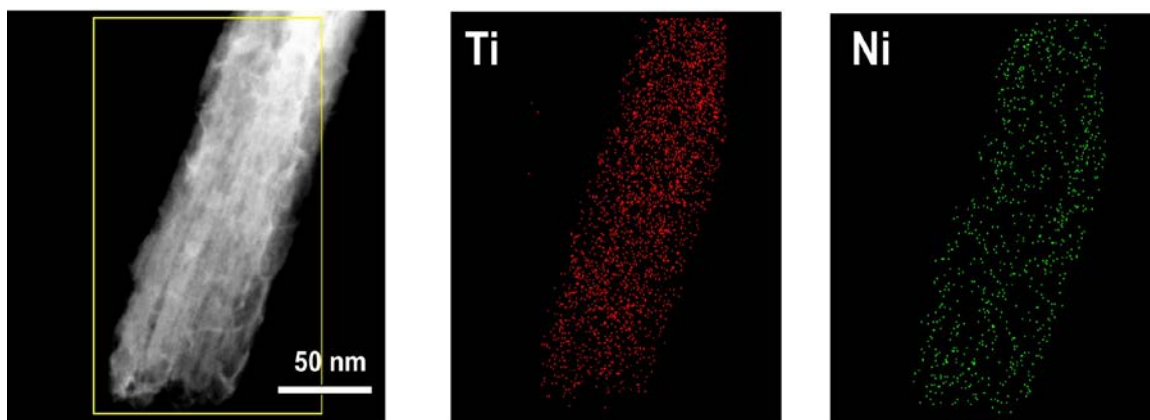


Figure S1. TEM image and the energy dispersive X-ray spectroscopy (EDX) elemental mappings of Ti and Ni of TiO_2/NiO composite.

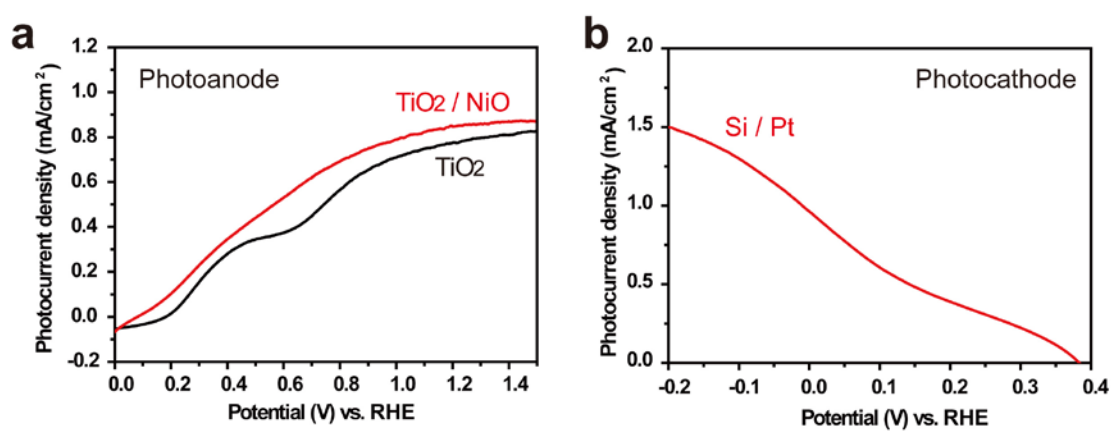


Figure S2. Photocurrent densities of (a) TiO_2 NW and TiO_2/NiO photoanodes, and (b) Si/Pt photocathode, using the 3-electrode configuration in 0.5 M Na_2SO_4 electrolyte.

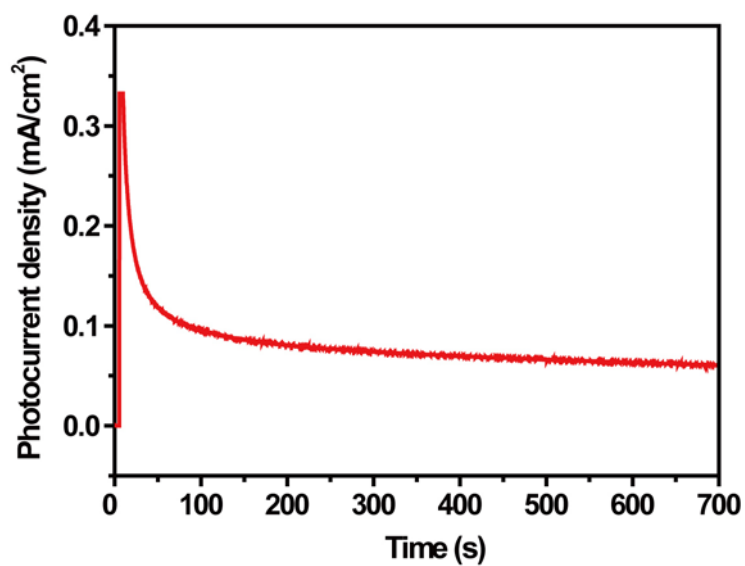


Figure S3. Photocurrent density versus time measured at short-circuited connection of the TiO₂/NiO photoanode and Si/Pt photocathode.

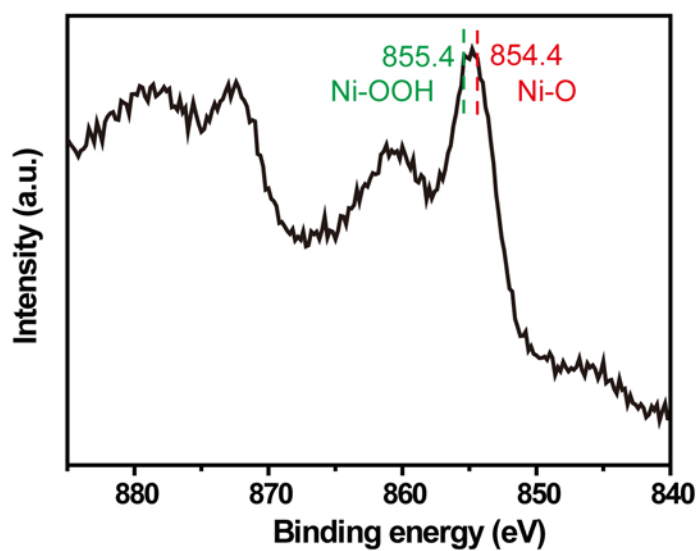


Figure S4. XPS spectra of the TiO₂/NiOOH photoanode. The Ni 2p_{3/2} peaks are indicated by arrows.

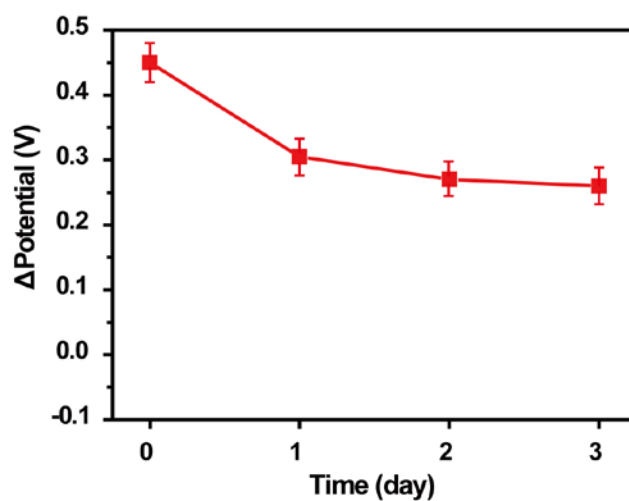


Figure S5. Open circuit voltage stability of the $\text{TiO}_2/\text{NiOOH}$ sample after fully charged by sun light.

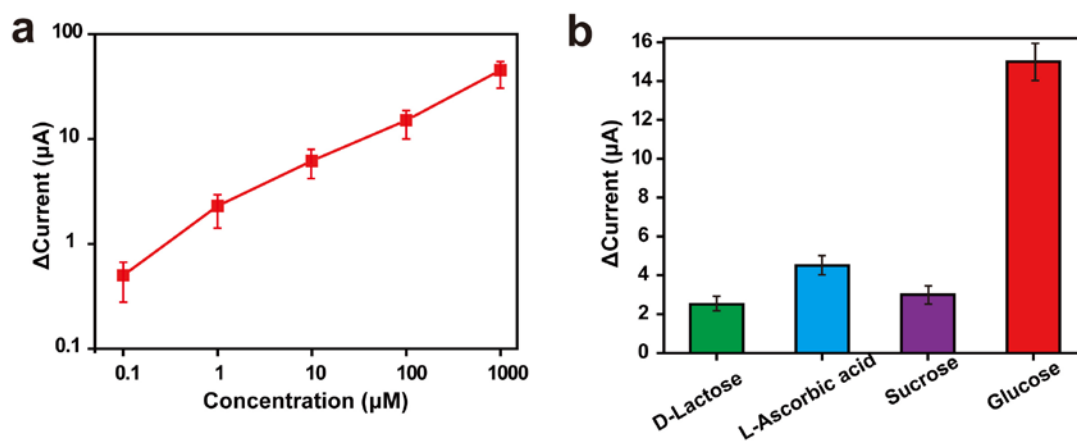


Figure S6. (a) Concentration dependence curve of the glucose detection by the TiO_2/NiO photoanodes under the sun light illumination. (b) Glucose selectivity compared to D-lactose, L-ascorbic acid, and sucrose, for the TiO_2/NiO photoanodes.